Synthesis, Characterization and Evaluation of Amphoteric Galactomannan Derivative for the Mitigation of Malachite Green and Congo Red Dye From Aqueous Solution

Deepak Sharma
Forest Research Institute Dehradun
Vineet Madan
Forest Research Institute Dehradun
Pradeep Sharma (drsharma27@gmail.com)
Forest Research Institute Dehradun https://orcid.org/0000-0002-5960-5931

Research Article

Keywords: Biopolymer, Dyes, Galactomannan, Adsorption, Dyes, Polysaccharide

Posted Date: April 5th, 2021

DOI: https://doi.org/10.21203/rs.3.rs-352705/v1

Version of Record: A version of this preprint was published at Cellulose on January 14th, 2022. See the published version at https://doi.org/10.1007/s10570-021-04332-5.

Synthesis, characterization and evaluation of amphoteric galactomannan derivative for the mitigation of malachite green and congo red dye from aqueous solution

Deepak Sharma[a], Vineet Kumar[a], and Pradeep Sharma[a*]

[a]Chemistry and Bioprospecting Division
Forest Research Institute Dehradun-248006
Indian Council of Forestry Research and Education

Abstract

Biopolymeric materials have been utilized for water treatments since ancient times. Consequently, there is a cumulative and persistent interest in the study of novel sustainable, inexpensive and natural biobased alternatives. Amphoteric derivatives of galactomannans are still unexplored and rarerly used materials to treat industrial wastes. The study was explored to synthesize and characterize amphoteric derivative of *Cassia tora* gum, a 1,5 galactomannan for its application as a potential adsorbent for mitigation of cationic (Malachite green) and anionic (Congo red) dyes by applying 'Taguchi design' (L9). The derivative was also studied for the conditioning of water using kaolin suspension. The results indicated that amphoteric derivative (anionic DS ~ 0.52 and cationic DS 0.197) is effective in maximum adsorption of Malachite green (73%) and Congo red (17 %) dyes and as a flocculant at a minimum dose of 10 ppm. The amphoteric derivative was characterized by X-ray-diffraction, TG analysis and spectroscopic techniques.

Keywords: Biopolymer, Dyes, Galactomannan, Adsorption, Dyes, Polysaccharide

---

Corresponding author: Chemistry and Bioprospecting Division, Forest Research Institute Dehradun-248006, Uttarakhand, India
E-mail addresses: drsharma27@gmail.com; sharmap@icfre.org (Pradeep Sharma).

1. Introduction

The developing concerns of water scarcity and environmental sustainability consciousness have renewed the global awareness towards the functional reuse and treatment of extremely contaminated wastewater (Grant et al., 2012). Water pollution caused by synthetic dyes and its threat on environment has significantly attracted the worldwide attention (Xie et al., 2014). Water soluble dyes possessing cationic, anionic, and non-ionic groups are widely being used in diverse industrial segments leading to water pollution due to their persistent growth and progress in numerous industries such as textiles, leather, paper production, pharmaceutical and food technology etc (Gupta, 2009; Chen et al., 2009; Gharbani et al., 2009; Cripps et al., 2009; Karadag et al., 2006; Reed et al., 1998). According to a report >50000 ton of dye is released in dyeing process causing serious environmental threat (Blackburn, 2009). The presence of dyeing effluent in a watercourse has a severe environmental impact as they are highly visible, non-biodegradable, toxic, and further, potentially able to be transformed into carcinogenic, teratogenic, and even mutagenic agents, creating a serious threat to human health and marine organisms (Sansuk et al., 2016). In the textile industry, generation of wastewater is chemically contaminated with dyestuffs, inorganic salts and other chemicals (Han et al., 2017). The release of such extremely contaminated wastewater into aquatic environments not only causes deleterious consequences to the aquatic ecosystems and public health yet additionally decreases the measure of accessible water. The unceasing exposure of colouring matter and their intermediates are responsible carcinogens and to a lesser extent sensitizers and allergens (Horng & Huang, 1993). Malachite green (MG), a cationic dye and Congo red (CR), an anionic dye are water soluble dyes and consistently used in the textile and paper industries (Kolya & Tripathi, 2013; Rao, 1995; Becki et al., 2008; Ahmad & Kumar, 2010). Intriguingly, these dyes are harmful due to their toxic and carcinogenic thrust

and as a liver tumour promoter to the mammals (Srivastava et al., 2004; Culp & Beland; 1996; Rao, 1995).

The effective treatment and retrieval of the severely polluted water before returning to the biological system have become a significant issue. Therefore, efficient methods of separation and removal of water contaminants are required to cope with hazardous situation (Sansuk, 2016; Han, 2016). In principle, diverse methods are utilized for decolouration viz.: , coagulation, biodegradation, chemical degradation, and photodegradation (Bouaziz, 2017). Further, reducing the turbidity of industrial and municipal waste water by coagulation–flocculation treatment is a well-known process. The polymers with anionic and cationic amalgamation have been used in the coagulation–flocculation process to reduce coagulant dosages, the volume of sludge and the ionic load of the waste-water and further, to reduce overall costs (Yan et al., 2009; Larsson & Wall, 1998; Ovenden & Xiao, 2002; Sirviö et al., 2011). Generally synthetic polymers viz., poly-acrylamides, polyacrylic acids, and poly-styrene sulphonic acid and their derivatives are used in coagulation-flocculation treatments which are not readily biodegradable and also behave as neurotoxic and carcinogenic (Suopajärvi, 2013; Suopajärvi et al., 2014). Alternatively, green biopolymers viz. starch, guar gum, chitin, pectin and algin, and their derivatives have been studied as biopolymeric materials, for the treatment of wastewater as dye adsorbent and flocculants due to their biodegradable nature and safe to human beings (Wang et al., 2013).

The galactomannan obtained from the seeds of *C. tora* Linn. a ruderal species (Family: *Leguminosae*; subfamily: *Caesalpiniaceae*(Pawar&D'mello, 2011; Sharma et al., 2020a; Sharma et al., 2020b) is of developing interest because of its non-toxicity, safety, biodegradability, biocompatibility, renewability and sustainability (Thombare et al., 2016). It possesses main chain comprised of (1→4)-β-D-mannopyranose (Man) units which are attached to (1→6)-α-D-galactopyranose (Gal) units with M: G, 5:1 (Hallagan et al., 1997). *C.*

tora gum has owned its limitations due to its unique structure and performance thereof in its native form. The functional properties of the galactomannans significantly affect the degree of their application. Incorporation of new functional moieties onto the galactomannans intensifies ingenious property, polarity and hydrophilicity, which enhance the interaction of the gum with various compounds. Quaternization and carboxymethylation are well-known derivatization processes for imparting the new functional properties to the galactomannans. Quaternization and carboxymethylation of polysaccharides viz. cellulose, starch, chitosan and galactomannans, are regarded as safe strategy to synthesize functional polysaccharides to impart new distinctive characteristics like high water solubility, antibacterial activity, and conditioning property in hair styling products, anionic dye capacity and flocculant in waste water treatments (Novac et al., 2014), and hydrophilicity, solution clarity, stability in aqueous systems and to enhance biological activities by changing their molecular structure, dye adsorbent and flocculant in waste water treatments (Thombare et al., 2016; Dodi et al., 2011; Heinze & Koschella, 2005; Huang et al., 2016; Xu et al., 2019; Narayanan et a., 2014; Rahul et al., 2014).

The present study aimed to assess the perceived design and synthesis of a water-soluble hybrid novel amphoteric derivative of *C. tora* gum (CMQCTG), having the amalgamation of both anionic and cationic nature, for removal of cationic (MG) and anionic (CR) dyes and as a flocculant over a dispersion of kaolin in water. A systematic statistical design i.e., Taguchi 'L9' was used to conduct the experiment for optimizing the parameters viz. adsorbent dosage, temperature, and time for the dye removal process. The synthesized amphoteric product was characterized by ^{1}H, ^{13}C, DEPT-135, HSQC NMR, FTIR, FESEM, X-ray diffraction, and TG analysis.

2. EXPERIMENTAL SECTION

2.1. Materials

C. tora gum was procured from M/s Goodrich Cereals Haryana, India. The quaternizing reagent 3-chloro-2-hydroxypropyltrimethylammonium chloride (CHPTAC, 60 wt. % aqueous), and deuterium oxide were procured from Sigma-Aldrich, St. Louis, Missouri, USA. Monochloroacetic acid (MCA), sodium hydroxide, isopropanol, methanol, and acetic acid were purchased from Merck India Ltd., Mumbai, India. Malachite green, Congo red dye and Kaolin extra pure was purchased from Loba Chemie Pvt. Ltd.

2.2. Methods

2.2.1. Synthesis of carboxymethyl and quaternized *Cassia tora* gum (CMQCTG)

C. tora gum (CTG, 100 mesh, 0.03075 mol) was dispersed in aqueous alkaline (0.15 mol) isopropanol solution (isopropanol: water, 80:20, v/v). The reaction flask was kept on a magnetic stirrer for continuous stirring at a temperature 50°C. After 10 minutes, MCA (0.0396, mol) was added in parts and continuous stirred for 60 min. To this reaction mixture (pH 12.9) CHPTAC (0.00478-0.0319 mol) was added and the reaction mixture was further stirred for 240 min (Sharma et al., 2020a). Intriguingly, the pH depends upon the addition of varying amount of CHPTAC, therefore, the pH of the reaction mixture was measured during and after the completion of each reaction. The reaction product was filtered under vacuum after designated reaction time, dispersed in distilled water and an aqueous acetic acid (5%, v/v) was added drop wise to neutralize the solution. The neutralized reaction mixture was subjected to precipitation with methanol. The precipitated product was separated by centrifugation (15000 rpm for 12 min) followed by washing with 80% aqueous methanol (3x20 mL) and finally with pure methanol. The purified dual derivative (CMQCTG) was dried in the oven at 60˚C for 6 hrs.

2.2.2. Preparation of Malachite green (MG) and Congo red (CR) solution for optimizing adsorption capacity of CMQCTG

Stock solution of MG and CR (100 ppm) was prepared by dissolving 0.1 g of dye into 1.0 L distilled water (Koyla & Tripathy, 2013). Calibration curves for MG and CR (5 to 25 ppm) were prepared to determine the concentration of residual dyes in the experiments. The concentration of dye in the experimental solutions was determined by UV–VIS spectrophotometer (Chemito-2700) at λmax 617 and 495 nm respectively. Analysis was carried out using the CMQCTG as a cationic and anionic adsorbent. Taguchi L9 array, a statistical design of experiment was used for optimizing the parameters for MG and CR. The operating variables like degree of substitution (DS), amount of adsorbent, temperature, and contact time were the four factors with three sub levels for optimization process. For dye experiments, CMQCTG, (cationic DS, 0.023, 0.123, &0.197; anionic DS, 0.52) with different dose amount (10, 25, & 50 mg) was added to a 30 mL of dye solution (25 ppm) in a100 mL beaker. The dye solution was stirred for a stipulated time (60, 120, & 190 min) and temperature (25, 35, & 45°C). Finally, the solution was allowed to settle for five minutes. The supernatant liquid at half the height of the beaker was taken for the analysis by UV–VIS spectrophotometer. The percentage of dye was calculated using the formula given in eqn no 1.

$$Adsorption\ \% = \frac{(Co - Ce)}{Co} * 100 \qquad (1)$$

Where *Co* is the initial dye concentration, *Ce* is the final concentration obtained after adding the adsorbent.

2.2.3. Flocculation Test

Flocculation performance of the CMQCTG was carried out using Coagulation-Flocculation jar tests (Bratby, 1980). A suspension of kaolin in water (1%, w/v) was dispersed in five 250

mL beakers. The CMQCTG (10-50 ppm) was added to the beakers. Immediately after the addition of the CMQCTG, all the suspensions were stirred using magnetic bars at a constant speed of 100 r/min for 2 minutes followed by a slow agitation at 50 rpm for 5 minutes (flocculating time). The flocs were then allowed to settle down for 2 minutes (sedimentation time). At the end of the settling period, the absorbance of supernatant liquid at half the height of the clarified layer was measured using a UV-VIS spectrophotometer (Chemito-2700) at 670 nm.

3. CHARACTERIZATION OF CMQCTG

3.1. Elemental analyses

The nitrogen content of CMQCTG samples was determined by the Kjeldahl method.

3.2. Determination of degree of substitution (DS)

The DS for quaternisation of all the CMQCTG samples was determined on the basis of an increase in nitrogen content using the following formula (Heinze et al., 2004):

$$DS = \frac{162.2 \times \%\ \text{Nitrogen}}{1401 - 151.6 \times \%\ \text{Nitrogen}} \qquad \ldots\ldots\ldots (2)$$

The DS for carboxymethylation was determined according to a reported method with minor modifications (ASTM D1439-15, 2015). CMQCTG (500 mg) was converted into acid form by treating with 0.1M aqueous methanolic HCl (methanol:water::90:10, 50mL) in a 250 mL beaker with continuous stirring for 2 hrs. The solution was filtered and washed under suction using a G-4 sintered glass funnel with aqueous methanol (methanol: water::90:10, 8x20 mL) and finally with pure methanol. The resulting sample was dried in the oven at 100°C for 1hr and kept in a vacuum desiccator. The desiccated sample (250 mg) was dispersed in double distilled water (100mL) and treated with alkaline solution (10 mL, 0.1M NaOH) in a 250 mL conical flask. The flask was kept for stirring at 70°C until a clear solution (20-30 min)

obtained. The solution at this stage was titrated with 0.1M HCl using phenolphthalein as an indicator. The degree of etherification (G) was calculated as follows:

$$A = \frac{(BC - DE)}{F} \quad \ldots\ldots\ldots (3)$$

Where;

A = milliequivalents of acid consumed per gram of sample

B = NaOH solution added, mL

C = molarity of NaOH solution added

D = HCl required for titration of excess NaOH, mL

E = molarity of HCl

F = weight of CMCTG, g

$$G = \frac{0.162\ A}{(1 - 0.0584A)} \quad \ldots\ldots (4)$$

Where;

162 = gram molecular mass of anhydroglucose unit of CTG, and

58 = net increase in molecular mass of anhydroglucose unit for each carboxymethyl group substituted.

3.3. Infrared spectroscopy

FT-IR spectra were recorded on a Fourier transform infrared (FT-IR) spectrophotometer (Perkin Elmer-Spectrum II). Samples (2-3 mg) were blended with spectroscopic KBr powder (100 mg) and pellets prepared for recording the spectrum. The spectra were acquired by the accumulation of 16 scans, with a resolution of 4 cm^{-1}, at 400-4000 cm^{-1}.

3.4. ^{1}H, ^{13}C, DEPT-135 and 2D NMR (HSQC) spectroscopy

The NMR spectra of CTG and CMQCTG were acquired using a 500MHz Bruker spectrometer at 25°C. The samples were hydrolysed prior to recording the spectra. CTG (0.5

g) was treated with aqueous sulfuric acid solution (20%, 50 mL) and stirred for 30 min at 50°C. After cooling in a water bath, the reaction mixture was neutralized by saturated sodium bicarbonate solution, and dialyzed against deionized water for 48hrs. The dialysate was filtered and freeze-dried. The freeze-dried sample (60mg) was dissolved in 1mL D_2O for NMR spectral analysis (Sharma et al., 2020a). Spectral recordings were performed at 303.3K using parameters- ^{1}H-NMR spectrum: 500.17 MHz, 32 scans, 2.2282 s data acquisition time, 1 s relaxation delay time; ^{13}C-NMR: 125.77 MHz, 1024 scans, 0.8847 s data acquisition time, 2 s relaxation delay time; DEPT-135: 512 scans, 0.8847 s data acquisition time, 2 s relaxation delay time; HSQC: 2 scans, 0.1946 s data acquisition time and 1.500s relaxation delay time.

3.5. Thermogravimetric analysis

Thermogravimetric analysis was carried out using ~3 mg of sample in a DTG-60 unit (Shimadzu, Japan) under nitrogen atmosphere with a flow rate of 40 mL/min. The scan was carried out at a heating rate of 10°C/min from 0°C to 800°C.

3.6. X-ray diffraction (XRD) analysis

XRD patterns of powdered samples were acquired using a Bruker D8 Advance (Germany) diffractometer (30 kV, 30 mA) equipped with Cu Kα radiation at a wavelength of (λ=1.5418Å). The relative intensity was recorded in the scattering range (2θ) of 0–90° at the scanning rate of 2°/min.

3.7. Field emission scanning electron microscopy (FESEM)

The field emission scanning electron microscopy was used to study the morphology of CTG and CMQCTG using instrument MIRA3 TESCAN, USA. The sample was mounted on a circular aluminium stub with double sticky tape, coated with gold and the images of samples were captured with an accelerating potential difference of 10kV at a working distance of 5 mm.

4. RESULTS AND DISCUSSIONS

The synthesis of amphoteric derivative proceeds consecutively via Williamson's ether synthesis (Scheme 1) (Su et al., 2019). The substitution of sodium carboxymethyl and quaternary ammonium moiety onto CTG was achieved by etherification, where the alkoxide ion reacts with the MCA and subsequently with the EPTAC (2,3-epoxypropyltrimethylammonium chloride), produced in situ from CHPTAC leading to formation of the amphoteric product (CMQCTG) comprising of carboxymethyl and quaternary ammonium groups. The maximal degree of substitution is achieved when all hydroxyl groups are etherified, however, during the reaction sodium glycolate and 2,3-dihydroxypropyltrimethylammonium chloride are also formed as by-products simultaneously affects the DS (Sharma et al., 2020a; Su et al., 2019).

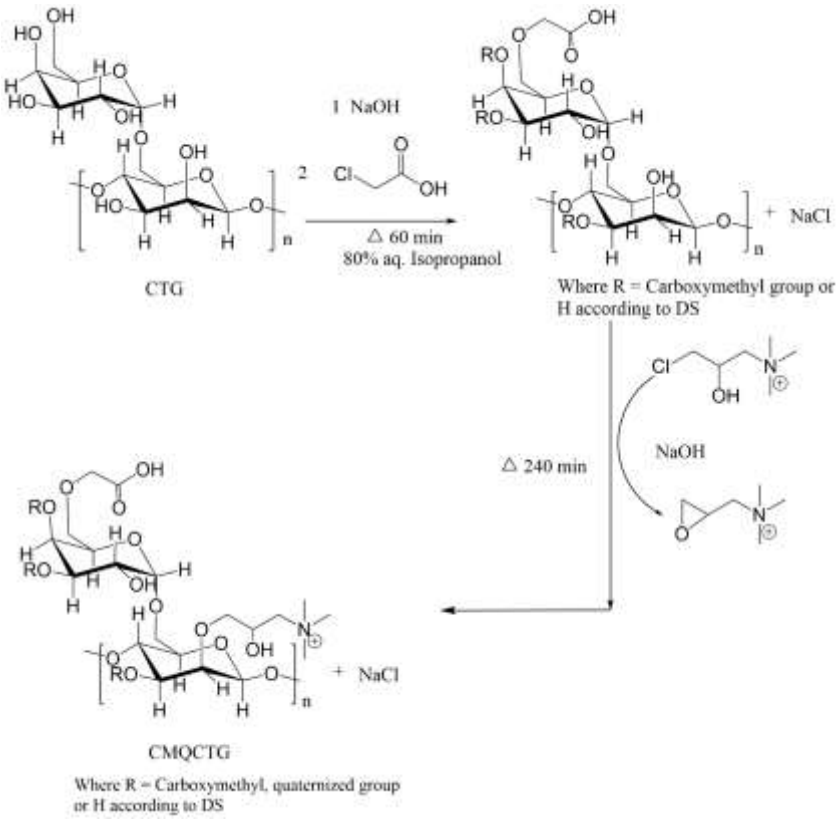

SCHEME1. Synthesis of amphoteric derivative

Table 1. Reaction Parameters and their Influence on Degree of Substitution

Gum (mol)	Time (hr)	Alkali (mol)	MCA (mol)	Temperature (°C)	Gum: Solvent	DS*	CHPTAC (mol)	pH	DS**
0.03075	1	0.15	0.0396	50	01:20	0.53	0.00478	12.9	0.023
0.03075	1	0.15	0.0396	50	01:20	0.54	0.00797	12.73	0.0307
0.03075	1	0.15	0.0396	50	01:20	0.51	0.01196	12.6	0.0972
0.03075	1	0.15	0.0396	50	01:20	0.50	0.0159	12.5	0.123
0.03075	1	0.15	0.0396	50	01:20	0.62	0.0199	12.35	0.142
0.03075	1	0.15	0.0396	50	01:20	0.58	0.0239	12.29	0.154
0.03075	1	0.15	0.0396	50	01:20	0.52	0.0319	12.2	0.197
*Degree of substitution (DS): Carboxymethyl derivative; **DS: Quaternized derivative									

The effect of CHPTAC concentration (0.00478–0.0319 mol) on the cationization of anionic CTG was studied in terms of the effect on DS and pH of reaction medium (Table 1). A distinct pattern was observed for the pH verses CHPTAC concentration (Fig.1). As the concentration of CHPTAC increases from 0.00478 to 0.0319 mol, the pH of the reaction medium decreases (12.9 to 12.2). A maximum of 0.2 DS for quaternization was achieved using 0.0319 mol of CHPTAC concentration at different reaction parameters studied. The increase in the cationic DS on increasing CHPTAC concentration may be due to the increased accessibility of the reactive groups (EPTAC) to the available alkoxide ions generated onto the galactomannan. Further, decrease in pH on increasing the concentration of CHPTAC may be due to utilization of available alkali with the CHPTAC and subsequently formation of EPTAC, as active species.

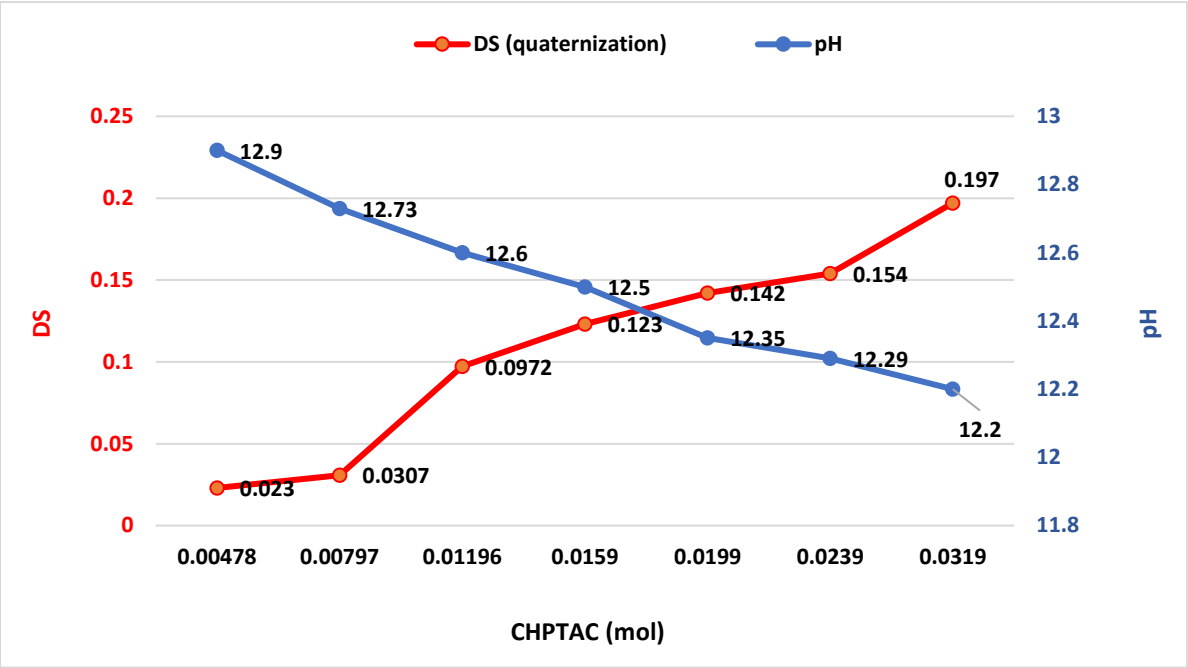

Fig. 1. Effect on DS (quaternisation) and pH on varying amount of CHPTA**C**

4.1. Characterization

Spectroscopic methods were used for structural analysis of CMQCTG. 1D and 2D NMR spectrum (Fig. 2) werer ecorded in order to confirm the incorporation of carboxymethyl substituent and quaternary ammonium groups onto CTG. In ^{1}H-NMR spectra, corresponding to α- and β- anomeric confirmers of galactose and mannose units, signals were observed in the region from 4.8 to 5.3 ppm (Bigand et al., 2011; Tako et al., 2018). The ^{1}H-NMR spectrum of CTG (Fig.2a) and CMQCTG (Fig. 2b) showed characteristic chemical shifts clustered between 3.3 ppm to 4.25 ppm for ring protons of mannose and galactose units. The occurrence of new peak of proton at 3.07 ppm in the spectra of CMQCTG was attributed to methyl protons (C-d, -$CH_2N(C\mathbf{H}_3)_3$) of quaternary ammonium groups and another downfield peak at 4.3 ppm was assigned to the methylene proton (-O-$\mathbf{CH}_2COO^-$) of carboxymethoxy substituents (Dodi et al., 2011).

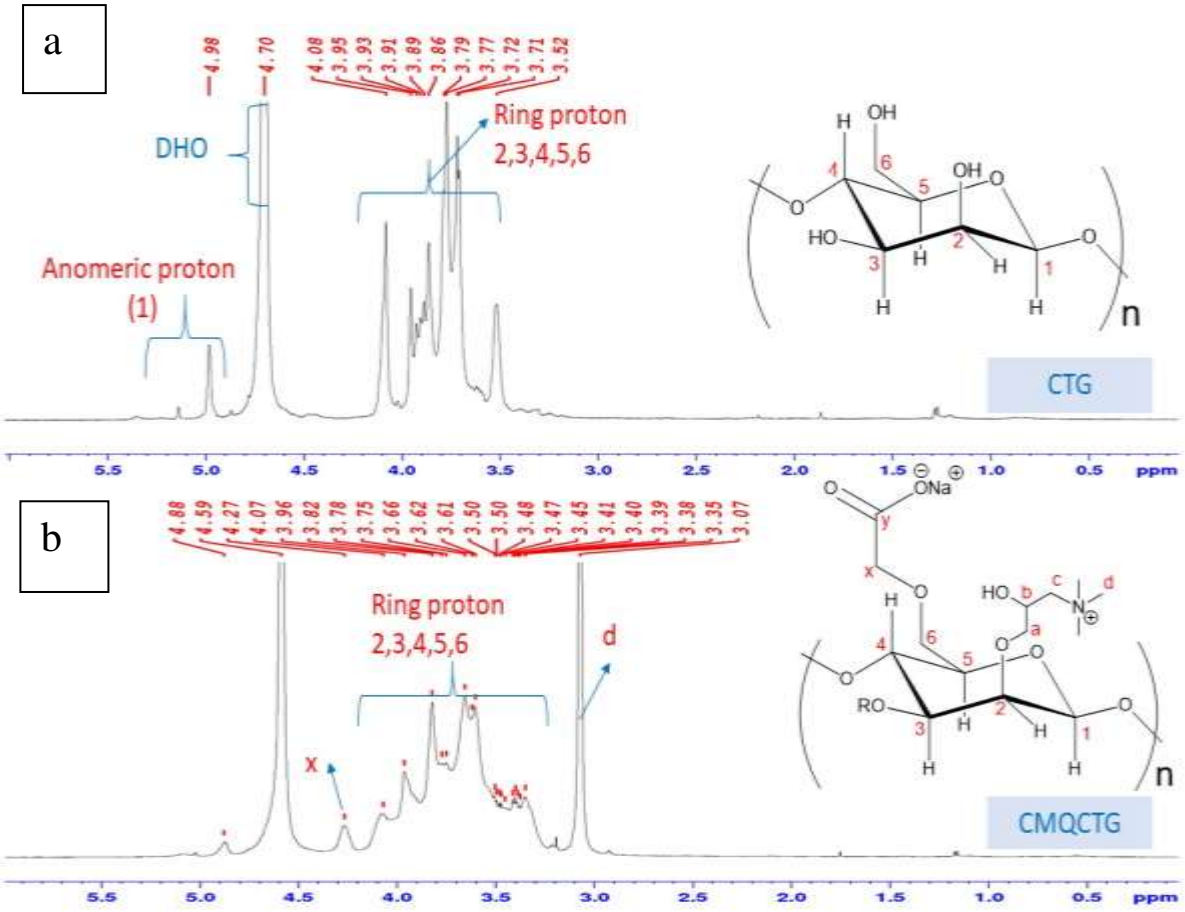
a
4.98
4.70
4.08
3.95
3.93
3.91
3.89
3.86
3.79
3.77
3.72
3.71
3.52
DHO
Ring proton
2,3,4,5,6
Anomeric proton
(1)
CTG
5.5
5.0
4.5
4.0
3.5
3.0
2.5
2.0
1.5
1.0
0.5
ppm
b
4.88
4.59
4.27
4.07
3.96
3.82
3.78
3.75
3.66
3.62
3.61
3.50
3.50
3.48
3.47
3.45
3.41
3.40
3.39
3.38
3.35
3.07
Ring proton
2,3,4,5,6
d
x
CMQCTG
5.5
5.0
4.5
4.0
3.5
3.0
2.5
2.0
1.5
1.0
0.5
ppm

267

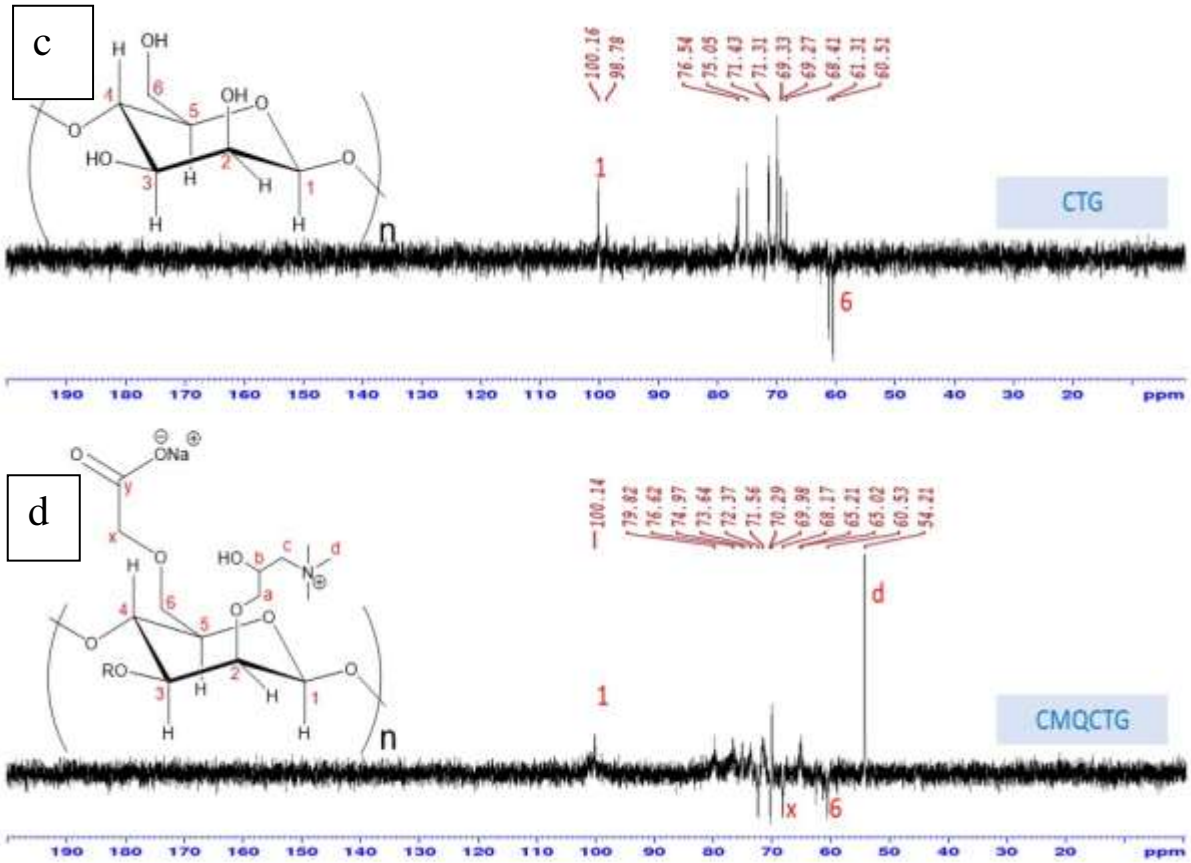
c
100.16
98.78
76.54
75.05
71.43
71.31
69.33
69.27
68.41
61.31
60.51
CTG
d
100.14
79.82
76.62
74.97
73.64
72.37
71.56
70.29
69.98
68.17
65.21
63.02
60.53
54.21
CMQCTG
ppm

268

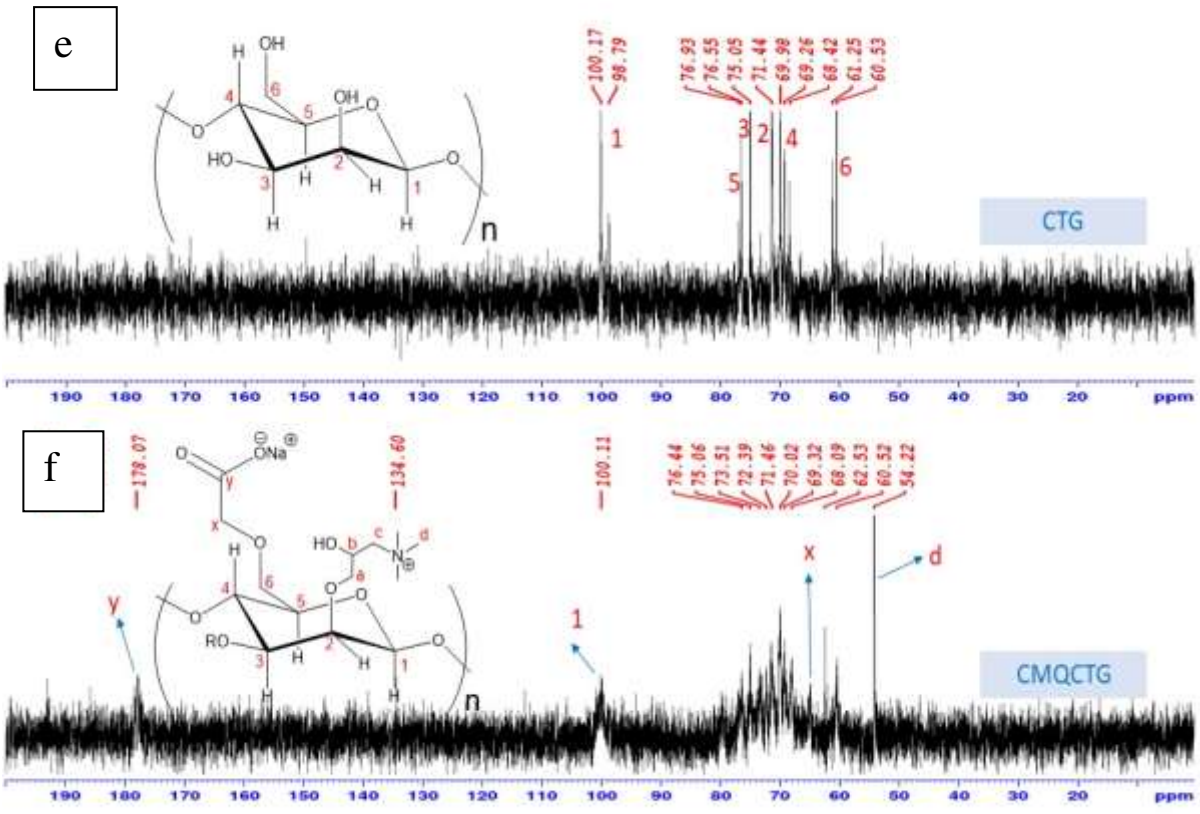
e
100.17
98.79
76.93
76.55
75.05
71.44
69.98
69.26
68.42
61.25
60.53
CTG
f
178.07
134.60
100.11
76.44
75.06
73.51
72.39
71.46
70.02
69.32
68.09
62.53
60.52
54.22
CMQCTG
ppm

269

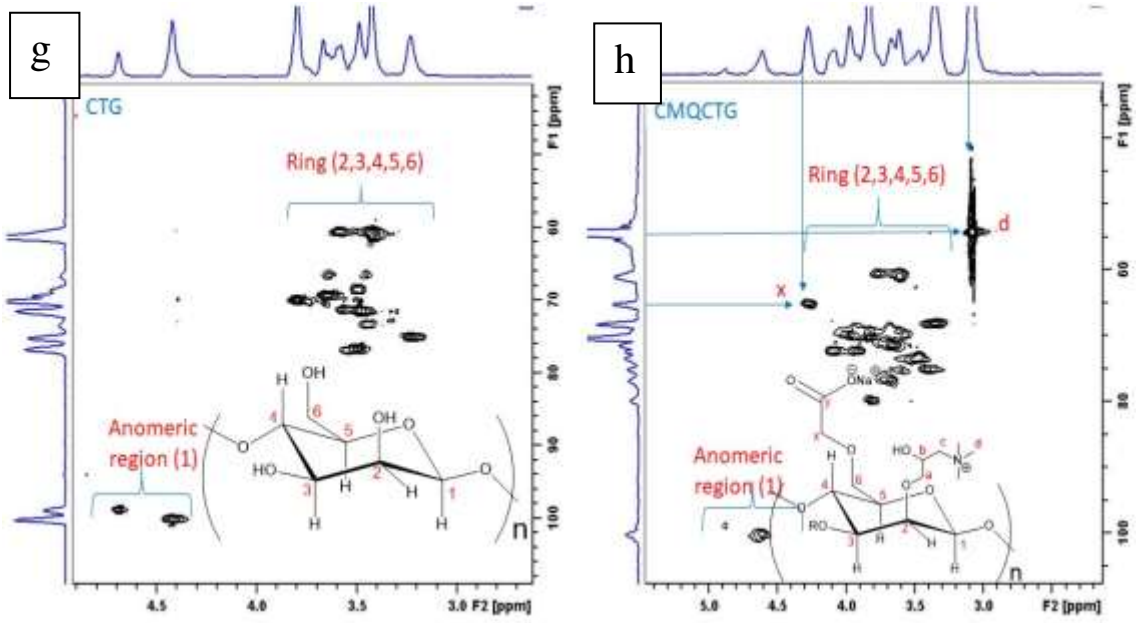

Fig. 2. NMR spectrum of CTG and CMQCTG: (a& b) ^{1}H-NMR spectrum; (c & d) ^{13}C-NMR spectrum; (e & f) DEPT Spectrum; (g & h) HSQC Spectrum

These two additional peaks in ^{1}H-NMR of CMQCTG confirm the incorporation of quaternary ammonium and carboxymethyl substituents onto galactomannan chain. The ^{13}C-NMR spectrum of CMQCTG (Fig.2d) showed three additional peaks in comparison to CTG (Fig. 2c). The prominent peak observed at 54.22 ppm was assigned to methyl carbons (-$CH_2N(\mathbf{C}H_3)_3$, C-d) of quaternary ammonium groups and the peak for methylene carbon (-$\mathbf{C}H_2N(CH_3)_3$, C-7) of carboxymethyl groups appeared at 68.09 ppm. The extreme downfield peak observed at 178.07 ppm can be assigned to the carboxyl (-$\mathbf{C}OO^-$) group at C-8 position. Further, the negative peaks appeared at 68.12 ppm and 60.53 ppm in DEPT-135 NMR (Fig. 2e & f) corroborates the presence of CH_2 groups on the carboxymethyl substituents (C-7) and carbon at C-6 (CH_2) position respectively. In addition, the correlation peaks (absence of signals in Fig. 2g) of carbon and hydrogen (Fig. 2h) for C-7 at 4.3 and 68.09 ppm and C-d at 3.07 and 54.22 ppm for ^{1}H & ^{13}C-NMR respectively confirms the presence of carboxymethyl and quaternary ammonium substituents in the amphoteric derivative.

FT-IR spectra were recorded to elucidate the structure of CTG and CMQCTG (Fig.3a). The broad band from 3600 and 3000cm^{-1} is attributed to O-H stretching frequency and it is due to

inter as well as intra molecular hydrogen bonding involving between the hydroxyl groups of the gum molecules. The band at 2919.6 cm^{-1} was assigned to characteristics symmetrical stretching vibrations due to the -CH_2 groups (Yuen et al., 2009). In native CTG the band at 1641.3 cm^{-1} was attributed to scissoring of two O-H bond of absorbed water molecule (Liu et al., 2012; Mudgil et al., 2012). The band appeared at 1025.8 cm^{-1} was due to the -C-O-C- stretching frequency of ether bond in the ring. The two other absorption bands at 814.6 cm^{-1} and 875.5 cm^{-1}can be assigned to α-D-galactopyranose and β-D-mannopyranose units of anomeric region respectively (Yuen et al., 2009; Figueiro et al., 2004; Prado et al., 2005). These characteristic peaks were also observed in the amphoteric derivative. In addition, four new absorption bands: 1475.7cm^{-1}, C-N stretching frequency of quaternary ammonium groups 1599.6 cm^{-1} (Pi-Xin et al., 2009; Banerjee e t al., 2009), -COO^- asymmetric stretching frequency; 1428.7 cm^{-1} and 1325.2 cm^{-1}, symmetric stretch of -COO^-group (Gong et al., 2012), were observed in the amphoteric derivative.

Wide-angle X-ray diffractogram of native gum showed the presence of diffraction peaks at 20° & 38° 2θ suggesting a semi-crystalline structure in nature (Fig. 3b). By contrast, in the XRD pattern of CMQCTG, the diffraction intensity has reduced and the peak shape switched from broad to diffuse peak indicating decrease in crystalline structure due to the incorporation of anionic and cationic groups (Wang & Xie, 2010). The cationic and anionic interaction also prevents the molecule acquiring complete amorphous structure. This decrease in crystalline structure may also be due to the alkaline medium during the reaction leading to interruption in intermolecular hydrogen bonding and consequently destruction in the crystalline structure. On the other hand, incorporated carboxymethyl and quaternary ammonium substituents onto the galactomannan resulting in a steric effect which reduces the formation of intermolecular hydrogen bonding and consequently, the gum molecules arrange in a semi-crystalline structure (Zhang et al., 2013).

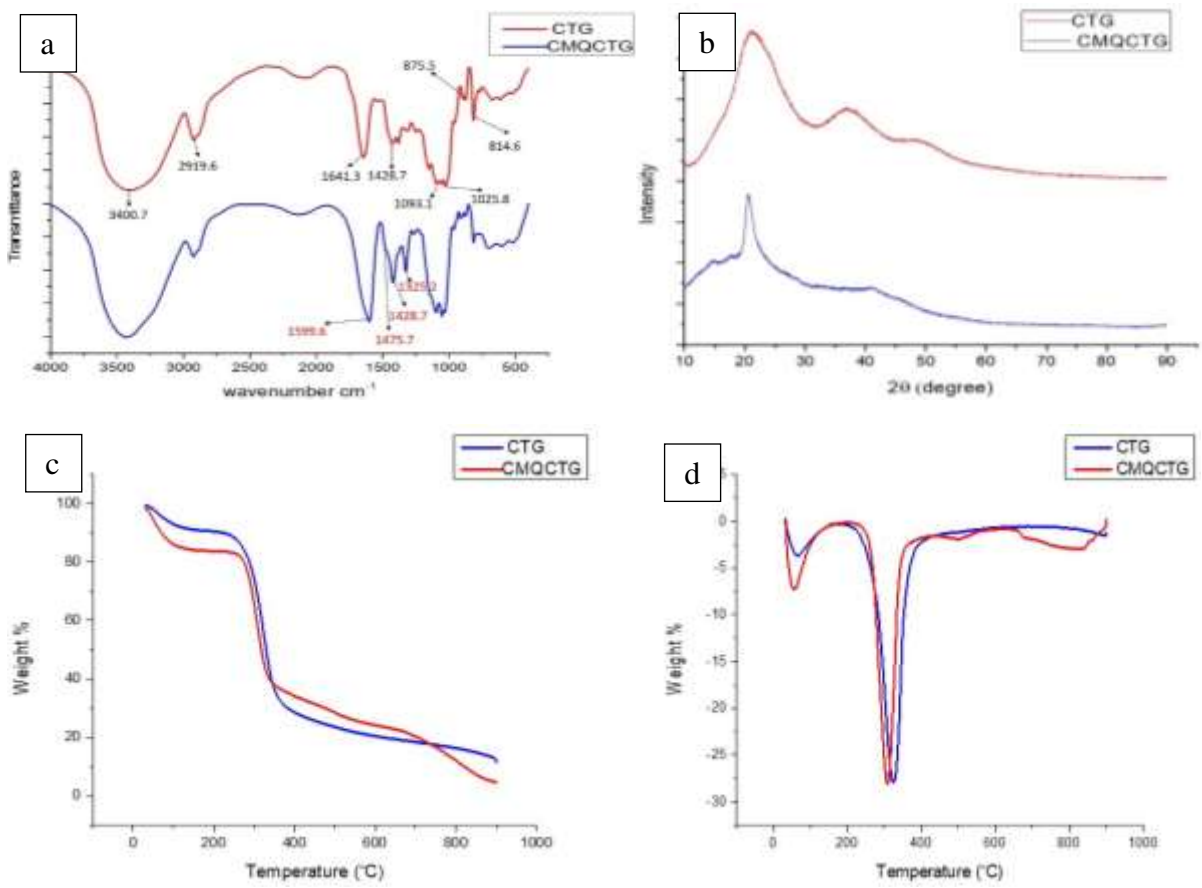

Fig.3. (a) FT-IR spectra of CTG & CMQCTG (b) XRD of CTG and CMQCTG (c) TGA of CTG & CMQCTG (d) DTG of CTG & CMQCTG

The results for TG and DTG for CTG and CMQCTG derivatives are presented in Fig. 3c & 3d which provides vital information about the thermal stability of polymeric material, such thermophysical information is of great use for industrial applications of polymer. The CTG and CMQCTG showed two stage weight losses up to 800°C. The first weight loss is due to the moisture content up to 125°C. The second weight loss is due to the decomposition of polysaccharide, water is main product of decomposition below 350°C. The CTG began to decompose at 250°C, and underwent 65% weight loss at 380°C. The studies indicate that the maximum degradation occurred within the range 240–410°C and the peak as indicated by the DTG (DTG_{max}) (Fig.3d) was at 335°C. Further heating from 450 to 800°C resulted in carbonization and ash formation. In case of CMQCTG, maximum degradation occurs within the range of 220 to 390°C with 45% of mass loss and the peak indicated by DTG (DTG_{max})

329 was at 315°C. There is very small difference in the final decomposition temperature for CTG
330 & CMQCTG but the percentage mass loss for CTG is greater than the CMQCTG. The lesser
331 percentage mass loss in case of CMQCTG (45%) in comparison to CTG (65%) indicating the
332 better thermal stability of amphoteric derivative. The initial decomposition temperature of
333 CMQCTG is lower than the initial decomposition temperature of the CTG. This may be due
334 to the substitution of the hydroxyl groups onto galactomannan chain with carboxymethyl and
335 quaternized ammonium groups which results in better thermal stability (Li et al., 2010).
336 The surface morphology of CTG and CMQCTG was studied using FESEM. The micrographs
337 showed the presence of smooth and well-defined particles of various sizes in CTG (Fig. 4 a)
338 whereas the surface morphology of CMQCTG (Fig. 4 b) altered markedly due to the insertion
339 of cationic and anionic moiety onto CTG.

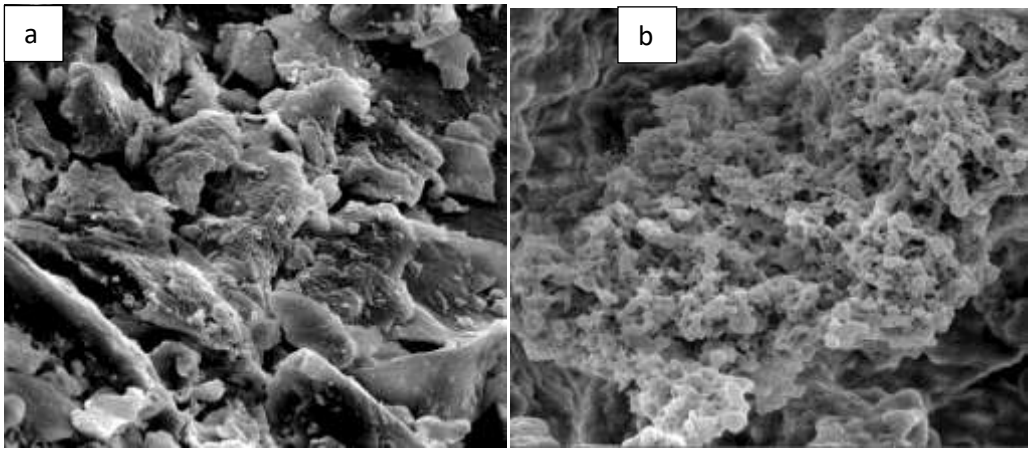

340

341 **Fig. 4.** (a) FESEM image of (a) CTG and (b) CMQCTG

342 Fig. 4 b shows the surface of CMQCTG which is completely disintegrated into a porous and
343 highly rough surface with devoid of well-defined edges. The incorporation of cationic and
344 anionic moieties disintegrates the particle shape and size consequently increasing the surface
345 roughness. In addition, the changes in the surface morphology of the CTG may also be due to
346 the increased cationic and anionic interaction and columbic repulsion in the molecular
347 structure as a result of the increased charge leading to disrupt the inter and intramolecular

hydrogen bonding. The chemical analysis and thorough spectroscopic studies showed that CTG was successfully derivatized into amphoteric derivative.

4.2. Adsorption study of malachite green and congored dyes by amphoteric derivative

The removal of Malachite Green (MG) and Congo red (CR) dyes was performed considering four factors viz. cationic DS, adsorbent amount, temperature, and contact time for optimization process. The effect of each parameter was assessed using Taguchi's experimental design comprising of a total of 9 experiments (Table 2) in terms of response values as percentage and signal to noise (S/N) ratios.

The *S/N* ratio was used to assess the quality characteristics of the product (Li et al., 2016; Tutar et al., 2014; Yang &Tarng, 1998). The highest *S/N* ratio signifies the optimum level for each factor and contributes to the maximum percentage.*S/N* ratio may be obtained by using equation 5.

$$\frac{S}{N}ratio = -10log_{10}\,(MSD) \qquad \ldots\ldots\ldots\ldots (5)$$

Where, MSD denotes the mean square deviation for output characteristic, and may be determined as (Eqn. 6).

$$MSD = \frac{1}{n}\sum_{i=1}^{n} 1/yi^2 \ldots\ldots\ldots\ldots\ldots (6)$$

Here, n represents the number of repetitions in the orthogonal array for the experimental design, and yi represents quality characteristic of the ith experiment. The average *S/N* ratio of each experiment for each factor is given in Fig.5.

Dyes comprising of positive and negative charge and their on the dual derivative is based on the ion exchange mechanism (Bouaziz et al., 2017), and indulge by the electrostatic attraction between amphoteric groups and the cationic and anionic dye molecules, $(MG)^+$ and $(CR)^-$. The carboxylic groups of carboxymethyl substituents (COO^-) present on CMQCTG binds to

the positively charged malachite green molecules. In case of anionic dye $(CR)^-$ there is an electrostatic force of attraction between the negatively charged surface of CR and positively charged quaternary ammonium groups present on the CMQCTG. This electrostatic force of attraction between the dye molecules and the CMQCTG results into the removal of dye from water by settling/precipitation on the surface.

4.2.1. Effect of amphoteric derivative on adsorption capacity of dyes

The effect of amphoteric derivative on the dyes was studied with respect to *S/N* ratio which is directly proportional to percentage of dyes. In the present study the anionic DS (0.5) was kept constant and the cationic DS was varied (0.012, 0.123, & 0.197). Increasing the cationic DS, there is not any perceivable effect due to the presence of unvarying anionic charge (DS 0.5) on the CMQCTG which form the bond with the cationic surface of MG dye, however, the *S/N* ratio increases with increase in cationic DS constantly leading to increase in adsorption of CR dye. The product with cationic DS (0.197) showed maximum percentage or *S/N* ratio for both MG & CR dye.

4.2.2. Effect of the amount of amphoteric derivative on adsorption capacity

The study of the of MG and CR on the CMQCTG was performed at a dose of 10 to 50 mg in the dye solution (25ppm) with respect to *S/N* ratio obtained from the Taguchi L'9 statistical design. The result shown in Fig.5, and 6 reveals that on increasing the amount of CMQCTG the adsorption of dyes (MG and CR) increases. The increase in adsorption of dyes may be due to the presence of additional sites for adsorption on increasing the concentration of the amphoteric derivative. A dose of 50 mg of absorbent showed maximum adsorption for the dyes.

4.2.3. Effect of temperature on adsorption capacity

The effect of temperature on the adsorption study with respect to *S/N* ratio was studied in the range of 25–45°C. On increasing the temperature, the *S/N* ratio decreased in the case of MG leading to a decrease in adsorption percentage. Whereas, in case of CR the maximum adsorption was observed at 35°C and thereafter it decreased. Therefore, at a temperature of 25°C and 35°C maximum adsorption was observed for MG and CR dyes respectively.

Table 2. Matrix layout of Taguchi L'9 and the adsorption percentage of MG and CR

Run	Factor				Results	
	Cationic DS	Dose amount (mg)	Temperature (°C)	Time (min)	%MG	% CR
1	0.197	50	35	60	63.20	16.88
2	0.123	10	35	120	51.20	7.00
3	0.023	25	35	90	50.60	4.56
4	0.023	10	25	60	53.40	3.32
5	0.197	10	45	90	48.80	10.48
6	0.123	50	25	90	60.00	4.56
7	0.023	50	45	120	72.60	3.76
8	0.123	25	45	60	56.60	3.12
9	0.197	25	25	120	66.00	12.80

4.2.4. Effect of contact time on adsorption capacity

The effect of contact time of CMQCTG and the dyes was studied with respect to *S/N* ratio using statistical design. The results reveal that on increasing the duration of time (60-120 min) the adsorption of dyes increased. Generally, it is a surface phenomenon so as the time increases the maximum active sites present on the dye surface gets attached to the adsorbent resulting into the settling/precipitation of dye. The 120 minutes was found as the optimized time for the maximum removal of MG & CR (Fig. 6).

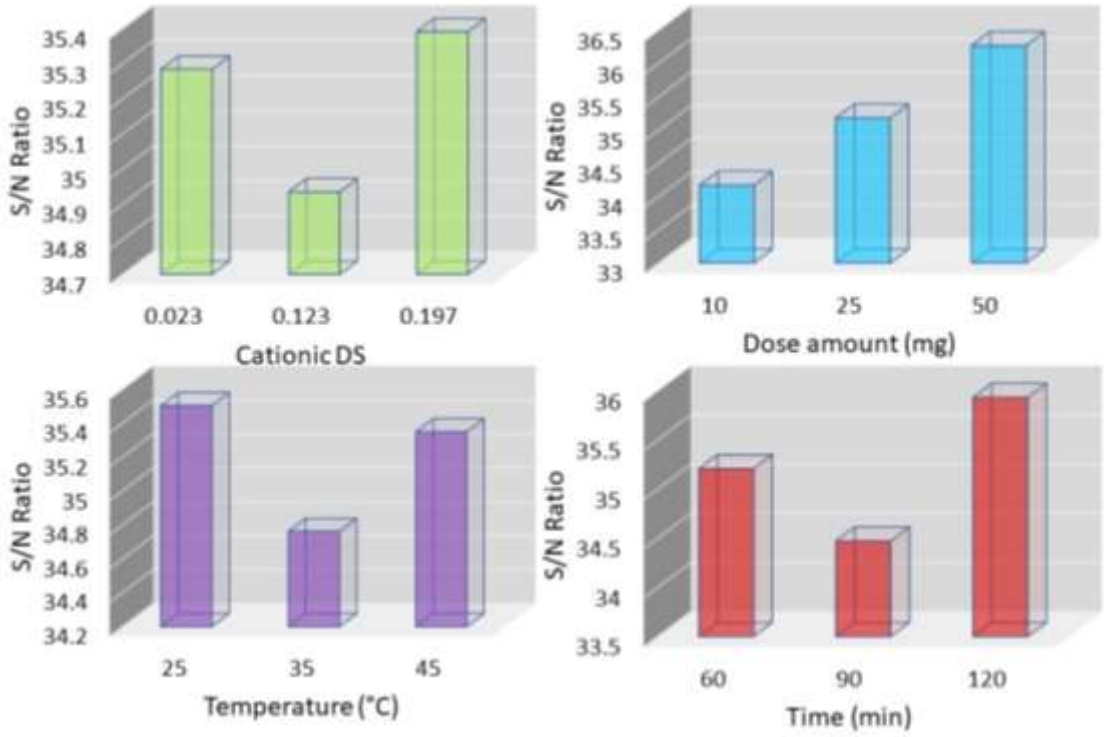

410

411 **Fig. 5.** Effect of different parameters on Malachite Green dyes with respect to *S/N* ratio

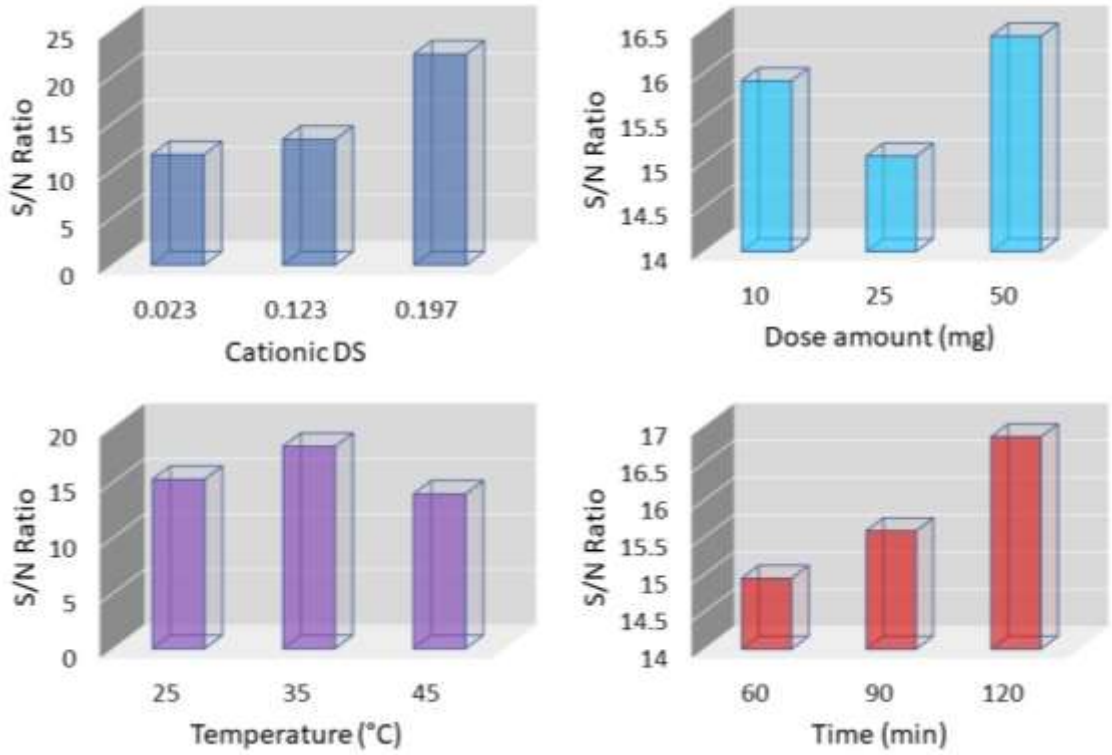

412

413 **Fig.6.** Effect of different parameters on Congo Red dyes with respect to *S/N* ratio

414 The experimental results (Fig. 5 and 6) suggest that these factors at the optimum levels
415 strongly support the maximum removal of MG and CR. The optimized reaction conditions in
416 case of MG are, cationic DS 0.197, adsorbent amount 50mg, temperature 25°C and time 120
417 min. Similarly, the optimized reaction conditions in case of CR are cationic DS 0.197,
418 adsorbent amount 50mg, temperature 35°C and time 120 min. A confirmatory experiment
419 was conducted over the optimized reaction conditions for MG and CR. The results reveal a
420 maximum removal of 73% MG and 17% CR dyes using CMQCTG which suggest that the
421 CMQCTG is an effective biopolymeric amphoteric derivative for the removal of both
422 cationic (MG) and anionic (CR) dyes from water.

423 **Table 3.** Comparison of the removal of cationic and anionic dyes onto various adsorbents.

Adsorbents	**Maximum capacity %**	**Dye investigated**	**References**
Amphoteric *Cassia tora* gum	73	Malachite green	Present work
Amphoteric *Cassia tora* gum	17	Congo red	Present work
Luffa cylindrica fibres	4.7	Methylene blue	Cengiz &Cavas, 2008
Almond gum	19.6	Malachite green	Bouaziz et al., 2017
Grass waste	45.7	Methylene blue	Hameed, 2009
Coffee husks	9.01	Malachite green	Baek, 2010
Sun flower seed hull	9.2	Methyl violet	Hameed, 2008
Broad bean peels	19.27	Malachite green	Hameed & El-Khaiary, 2008

Crosslinked Chitosan beads	9.35	Malachite green	Chiou, 2004
Untreated guava leaves	29.5	Methylene blue	Ponnusami et al., 2008
Solid waste of soda ash plant	66.7	Reactive red 231	Şener, 2008

424

425 **4.3. Flocculation characteristics**

426 The flocculation results of the amphoteric CMQCTG samples with cationic DS values (0.12,
427 0.197) on kaolin suspension were measured in terms of the absorbance of the supernatant
428 liquid and the results are shown in Fig.7. It was observed that the product with higher DS
429 (0.197) is a better flocculant in kaolin suspension than the product with lower DS (0.12) in all
430 concentrations. The effect was probably due to the electrostatic force of attraction between
431 the cationic quaternary ammonium groups present on the CMQCTG derivative and the
432 negatively charged particles of the kaolin suspension via bridging and charge neutralization
433 process (Cengi & Cavas, 2008). The present study shows that on increasing the concentration
434 of cationic samples from 10 to 50 ppm the absorbance increases, resulting in an increase in
435 the turbidity of the suspension consequently decreasing the flocculation efficiency. This
436 effect may be due to the surface charge of kaolin became positive due to the absorbance of
437 cationic gum; thus, on increasing the concentration of flocculant doses the phenomenon of
438 bridging becomes insignificant due to the higher electric positive charge which leads to
439 mutual electrostatic repulsion consequences redispersion of the aggregated particles. The
440 CMQCTG having high DS (0.197) shows better flocculation results at a minimum
441 concentration (10 ppm) in comparison to 0.12 DS. From the aforementioned results, it was
442 found that the flocculation performance of CMQCTG is significantly enhanced on

introduction of cationic groups with high DS and can be used potentially as an efficient flocculant in wastewater treatments.

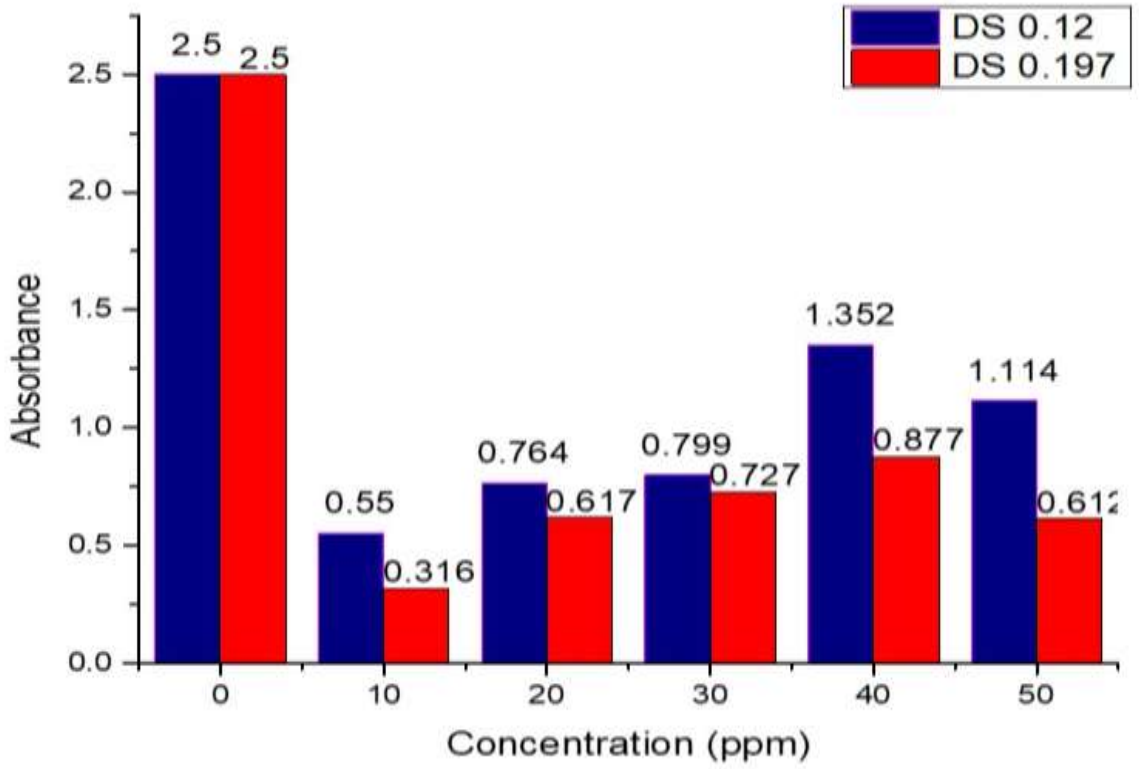

Fig. 7. Flocculation performance of CMQCTG

5. Conclusion

A novel biopolymeric, amphoteric derivative of *C. tora* gum was synthesized under heterogeneous conditions using monochloroacetic acid and 3-chloro-2-hydroxypropyltrimethyl ammonium chloride. The derivative was thoroughly characterized by spectroscopic techniques and investigated for its function and applicability in waste water treatments for cationic (MG) and anionic (CR) dyes. A systematic statistical design i.e., Taguchi' L'9 was used to conduct the experiment for optimization of dye process viz. adsorbent dosage, temperature, and time. The results reveal that 73% of MG and 17% of CR dye may be efficiently removed under stipulated conditions. The flocculation results demonstrated that the CMQCTG products have good flocculation efficiency over at

minimum concentration of dosages (10 ppm), and thus, it may be utilized as flocculant for wastewater treatment. The optimized reaction conditions for production of amphoteric derivative having DS of 0.52 and 0.197 for carboxymethylation and quaternization respectively were achieved using 0.0396 mol MCA , 0.15 mol NaOH, time 60min, 1:20 gum:solvent (80:20:: IPA: H_2O) ratio at 50°C for 0.03075, mol of CTG and 0.0319 mol CHPTAC, reaction time 60 and 240 min for carboxymethylation and quaternization respectivley. In conclusion, it may be deduced that the amphoteric derivative of *C. tora* gum is environmentally friendly biopolymer which has promising potential for removal of both cationic and anionic dyes from aqueous solutions and also as a potential flocculant for wastewater treatment.

Acknowledgments

The authors are grateful to the Director, Forest Research Institute (FRI), Dehradun for providing laboratory facilities. Authors gratefully acknowledge Sophisticated Analytical Instrumental Facility (SAIF), Panjab University, Chandigarh for recording spectral data.

Conflict of Interest

The authors declare that they have no conflicts of interest to declare that are relevant to the content of this article.

478 **References:**

479 Ahmad R, Kumar R (2010) Adsorption Studies of hazardous malachite green onto treated
480 ginger waste. J Environ Manage 91: 1032–1038. DOI:
481 10.1016/j.jenvman.2009.12.016

482 ASTM D1439-15 (2015) Standard Test Methods for Sodium Carboxymethylcellulose
483 ASTM International, West Conshohocken PA. www.astm.org

484 Baek MH, Ijagbemi CO, Se-Jin O, & Kim DS (2010) Removal of Malachite Green from
485 aqueous solution using degreased coffee bean. J Hazard Mater 176(1-3): 820-828. DOI:
486 10.1016/j.jhazmat.2009.11.110

487 Banerjee C, Ghosh S, Sen G, Mishra S, Shukla P, Bandopadhyay R (2013) Study of algal
488 biomass harvesting using cationic guar gum from the natural plant source as
489 flocculant. Carbohydr Polym 92(1): 675-681. DOI: 10.1016/j.carbpol.2012.09.022

490 Bekci Z, Özveri C, Seki Y, Yurdakoç K (2008) Sorption of malachite green on chitosan
491 bead. J Hazard Mater 154: 254–261. DOI: 10.1016/j.jhazmat.2007.10.021

492 Bigand V, Pinel C, Perez DDS, Rataboul F, Huber P, Petit-Conil M (2011) Cationisation
493 of galactomannan and xylan hemicelluloses. Carbohydr Polym 85(1): 138-148. DOI:
494 10.1016/j.carbpol.2011.02.005

495 Blackburn RS (2004) Natural polysaccharides and their interactions with dye molecules:
496 applications in effluent treatment. Environ Sci Technol 38(18): 4905-4909. DOI:
497 10.1021/es049972n

498 Bouaziz F, Koubaa M, Kallel F, Ghorbel RE, Chaabouni SE (2017) Adsorptive removal
499 of malachite green from aqueous solutions by almond gum: kinetic study and equilibrium
500 isotherms. Int J Biol Macromol 105: 56-65. DOI: 10.1016/j.ijbiomac.2017.06.106

501 Bouaziz F, Koubaa M, Kallel F, Ghorbel RE, Chaabouni SE (2017) Adsorptive removal
502 of malachite green from aqueous solutions by almond gum: kinetic study and equilibrium
503 isotherms. Int J Biol Macromol 105: 56-65. DOI: 10.1016/j.ijbiomac.2017.06.106

504 Bratby J (1980) Coagulation and flocculation. Uplands: Croydon England.

505 Cengiz S, &Cavas L (2008) Removal of methylene blue by invasive marine seaweed:
506 *Caulerpa racemosa* var. *cylindracea*. Bioresour Technol 99(7): 2357-2363. DOI:
507 10.1016/j.biortech.2007.05.011

508 Chen H, Xu H, Heinze TM, Cerniglia CE (2009) Decolorization of water and oil-soluble
509 azo dyes by *Lactobacillus acidophilus* and *Lactobacillus fermentum*. J Ind Microbiol
510 Biotechnol 36(12): 1459. DOI: 10.1007/s10295-009-0633-9

511 Chiou MS, Ho PY, & Li HY (2004) Adsorption of anionic dyes in acid solutions using
512 chemically cross-linked chitosan beads. Dyes and pigments 60(1): 69-84. DOI:
513 10.1016/S0143-7208(03)00140-2

514 Cripps C, Bumpus JA, Aust SD (1990) Biodegradation of azo and heterocyclic dyes by
515 *Phanerochaete chrysosporium*. Appl Environ Microbiol 56(4): 1114-1118.

516 Culp SJ, Beland FA (1996) Malachite green: a toxicological review. J Am Coll
517 Toxicol 15(3): 219-238. DOI: 10.3109%2F10915819609008715

518 Dodi G, Hritcu D, Popa MI (2011) Carboxymethylation of guar gum: synthesis and
519 characterization. Cellul Chem Technol 45(3): 171.

520 Figueiro SD, Góes JC, Moreira RA, Sombra ASB (2004) On the physico-chemical and
521 dielectric properties of glutaraldehyde crosslinked galactomannan–collagen
522 films. CarbohydrPolym 56(3): 313-320. DOI: 10.1016/j.carbpol.2004.01.011

523 Gharbani P, Tabatabaii SM, Mehrizad A (2008) Removal of Congo red from textile
524 wastewater by ozonation. Int J Environ Sci Technol 5(4): 495-500. DOI:
525 10.1007/BF03326046

526 Gong H, Liu M, Chen J, Han F, Gao C, Zhang B (2012) Synthesis and characterization of
527 carboxymethyl guar gum and rheological properties of its solutions. Carbohydr
528 Polym 88(3): 1015-1022. DOI: 10.1016/j.carbpol.2012.01.057

529 Grant SB, Saphores JD, Feldman DL, Hamilton AJ, Fletcher TD, Cook PL, Deletic A
530 (2012) Taking the "waste" out of "wastewater" for human water security and ecosystem
531 sustainability. Science 337(6095): 681-686. DOI: 10.1126/science.1216852

532 Gupta VK (2009) Application of low-cost adsorbents for dye removal–a review. J
533 Environ Manage 90(8): 2313-2342. DOI: 10.1016/j.jenvman.2008.11.017

534 Hallagan JB, La Du BN, Pariza MW, Putnam JM &Borzelleca JF (1997) Assessment of
535 Cassia gum. Food Chem Toxicol 35(6): 625-632. DOI: 10.1016/S0278-
536 6915(97)00018-5

537 Hameed BH (2008) Equilibrium and kinetic studies of methyl violet sorption by
538 agricultural waste. J Hazard Mater 154: 204–212. DOI: 10.1016/j.jhazmat.2007.10.010

539 Hameed BH (2009) Grass waste: A novel sorbent for the removal of basic dye from
540 aqueous solution. J Hazard Mater 166(1): 233-238. DOI: 10.1016/j.jhazmat.2008.11.019

541 Hameed BH, & El-Khaiary MI (2008) Sorption kinetics and isotherm studies of a cationic
542 dye using agricultural waste: broad bean peels. J Hazard Mater 154(1-3): 639-648. DOI:
543 10.1016/j.jhazmat.2007.10.081

544

Han G, Feng Y, Chung TS, Weber M, Maletzko C (2017) Phase inversion directly induced tight ultrafiltration (UF) hollow fiber membranes for effective removal of textile dyes. Environ Sci Technol 51(24): 14254-14261. DOI: 10.1021/acs.est.7b05340

Heinze T, Haack V, Rensing S (2004) Starch derivatives of high degree of functionalization. 7. Preparation of cationic 2-hydroxypropyltrimethylammonium chloride starches. Starch-Stärke, 56(7): 288-296. DOI: 10.1002/star.200300243

Heinze T, Koschella A (2005) Carboxymethyl ethers of cellulose and starch–a review. *In Macromolecular Symposia* March, (Vol. 223, No. 1, pp. 13-40). Weinheim: WILEY-VCH Verlag. DOI: 10.1002/masy.200550502.

Horng JY, Huang SD (1993) Removal of organic dye (direct blue) from synthetic wastewater by adsorptive bubble separation techniques. Environ Sci Technol 27(6): 1169-1175. DOI: 10.1021/es00043a017

Huang G, Chen X, Huang H (2016) Chemical modifications and biological activities of polysaccharides. Curr Drug Targets 17(15): 1799-1803.

Karadag D, Tok S, Akgul E, Ulucan K, Evden H, Kaya MA (2006) Combining and coagulation for the treatment of azo and anthraquinone dyes from aqueous solution. Ind Eng Chem Res 45(11): 3969-3973. DOI: 10.1021/ie060164+

Kolya H, Tripathy T (2013) Hydroxyethyl Starch-g-Poly-(N, N-dimethylacrylamide-co-acrylic acid): An efficient dye removing agent. Eur Polym J 49(12): 4265-4275. DOI: 10.1016/j.eurpolymj.2013.10.012

Larsson A, Wall S (1998) Flocculation of cationic amylopectin starch and colloidal silicic acid. The effect of various kinds of salt. Colloids Surf A 139(2): 259-270.DOI: 10.1016/S0927-7757(98)00326-4

Li L, Lv J, Chen W, Wang W, Zhang X, Xie G (2016) Application of Taguchi method in the optimization of swimming capability for robotic fish. Int J Adv Robot Syst 13(3): 102. DOI: 10.5772%2F64039

Li X, Gao WY, Huang LJ, Wang YL, Huang LQ, Liu CX (2010) Preparation and physicochemical properties of carboxymethyl *Fritillaria ussuriensis* Maxim. starches. CarbohydrPolym 80(3): 768-773. DOI: 10.1016/j.carbpol.2009.12.025.

Liu J, Ming J, Li W, Zhao G (2012) Synthesis, characterisation and in vitro digestibility of carboxymethyl potato starch rapidly prepared with microwave-assistance. Food Chem 133(4): 1196-1205. DOI: 10.1016/j.foodchem.2011.05.061

Mudgil D, Barak S, Khatkar BS (2012) X-ray diffraction, IR spectroscopy and thermal characterization of partially hydrolyzed guar gum. *Int J BiolMacromol* 50(4): 1035-1039. DOI: 10.1016/j.ijbiomac.2012.02.031

Narayanan D, Jayakumar R, Chennazhi KP (2014) Versatile carboxymethyl chitin and chitosan nanomaterials: a review. Wiley Interdiscip Rev: NanomedNanobiotechnol 6(6): 574-598, DOI.org/10.1002/wnan.1301.

Novac O, Lisa G, Profire L, Tuchilus C, Popa MI (2014) Antibacterial quaternized gellan gum-based particles for controlled release of ciprofloxacin with potential dermal applications. Mater Sci Eng C 35: 291-299. DOI: 10.1016/j.msec.2013.11.016

Ovenden C, Xiao H (2002) Flocculation behaviour and mechanisms of cationic inorganic microparticle/polymer systems. Colloids Surf A 197(1-3): 225-234, DOI: 10.1016/S0927-7757(01)00903-7

Pawar HA, D'mello PM (2011) *Cassia Tora* Linn.: An Overview. Int J Pharm Sci Res 2(9): 2286, DOI: 10.1016/j.tifs.2011.07.002

591 Pi-Xin W, Xiu-Li W, Xue DH, Xu K, Tan Y, Du XB, Li WB (2009) Preparation and
592 characterization of cationic corn starch with a high degree of substitution in dioxane–
593 THF–water media. Carbohydr Res 344(7): 851-855, DOI:
594 10.1016/j.carres.2009.02.023

595 Ponnusami V, Vikram S, & Srivastava SN (2008) Guava (Psidium guajava) leaf powder:
596 novel adsorbent for removal of methylene blue from aqueous solutions. J Hazard Mater
597 152(1): 276-286. DOI: 10.1016/j.jhazmat.2007.06.107

598 Prado BM, Kim S, Özen BF, Mauer LJ (2005) Differentiation of carbohydrate gums and
599 mixtures using Fourier transform infrared spectroscopy and chemometrics. J Agric Food
600 Chem 53(8): 2823-2829. DOI: 10.1021/jf0485537

601 Rahul R, Jha U, Sen G, Mishra S (2014) Carboxymethyl inulin: A novel flocculant for
602 wastewater treatment. Int J BiolMacromol 63: 1-7. DOI: 10.1016/j.ijbiomac.2013.10.015

603 Rao KV (1995) Inhibition of DNA synthesis in primary rat hepatocyte cultures by
604 malachite green: a new liver tumor promoter. Toxicol Lett 81: 107–113. DOI:
605 10.1016/0378-4274(95)03413-7

606 Rao KVK (1995)Inhibition of DNA synthesis in primary rat hepatocyte cultures by
607 malachite green: a new liver tumor promoter. Toxicol Lett 81(2-3): 107-113. DOI:
608 10.1016/0378-4274(95)03413-7

609 Reed BE, Matsumoto MR, Jensen JN, Viadero R, Lin W (1998) Physicochemical
610 processes. Water Environ Res 70(4): 449-473.

611 Sansuk S, Srijaranai S, Srijaranai S (2016) A new approach for removing anionic organic
612 dyes from wastewater based on electrostatically driven assembly. Environ Sci Technol
613 50(12): 6477-6484. DOI: 10.1021/acs.est.6b00919

614 Sener S (2008) Use of solid wastes of the soda ash plant as an adsorbent for the removal
615 of anionic dyes: equilibrium and kinetic studies. Chem Eng J 138: 207–214. DOI:
616 10.1016/j.cej.2007.06.035

617 Sharma D, Kumar V, Nautiyal R, Sharma P (2020b) Synthesis and characterization of
618 quaternized *Cassia tora* gum using Taguchi L'16 approach. Carbohyd. Polym 232:
619 115731. DOI: 10.1016/j.carbpol.2019.115731F

620 Sharma D, Kumar V, Sharma P (2020a) Application, Synthesis, and Characterization of
621 Cationic Galactomannan from Ruderal Species as a Wet Strength Additive and
622 Flocculating Agent. ACS omega 5(39): 25240–25252. DOI: 10.1021/acsomega.0c03408

623 Sirviö J Honka A, Liimatainen H, Niinimäki J, Hormi O (2011) Synthesis of highly
624 cationic water-soluble cellulose derivative and its potential as novel biopolymeric
625 flocculation agent. CarbohydrPolym 86(1): 266-270, DOI:
626 10.1016/j.carbpol.2011.04.046

627 Srivastava S, Sinha R, Roy D (2004) Toxicological effects of malachite green.
628 *AquatToxicol 66(3):* 319-329. DOI: 10.1016/j.aquatox.2003.09.008

629 Su L, Ou Y, Feng X, Lin M, Li J, Liu D, Qi H (2019) Integrated Production of Cellulose
630 Nanofibers and Sodium Carboxymethylcellulose through Controllable Eco-
631 carboxymethylation under Mild Conditions. ACS Sustainable Chem Eng 7(4): 3792-
632 3800. DOI: 10.1021/acssuschemeng.8b04492

633 Suopajärvi T, Koivuranta E, Liimatainen H, Niinimäki J (2014) Flocculation of municipal
634 wastewaters with anionic nanocelluloses: Influence of nanocellulose characteristics on
635 floc morphology and strength. J Environ Chem Eng 2(4): 2005-2012. DOI:
636 10.1016/j.jece.2014.08.023

637 Suopajärvi T, Liimatainen H, Hormi O, Niinimäki J (2013) Coagulation–flocculation
638 treatment of municipal wastewater based on anionizednanocelluloses. Chem Eng J 231:
639 59-67. DOI: 10.1016/j.cej.2013.07.010

640 Tako M, Tamaki Y, Teruya T (2018) Discovery of Unusual Highly Branched
641 Galactomannan from Seeds of Desmanthusillinoensis. J BiomaterNanobiotechnol 9(02):
642 101-116. DOI: 10.4236/jbnb.2018.92009

643 Thombare N, Jha U, Mishra S, Siddiqui MZ (2016) Guar gum as a promising starting
644 material for diverse applications: A review. Int J BiolMacromol 88: 361-372, DOI:
645 10.1016/j.ijbiomac.2016.04.001

646 Tutar M, Aydin H, Yuce C, Yavuz N, Bayram A (2014) The optimisation of process
647 parameters for friction stir spot-welded AA3003-H12 aluminium alloy using a Taguchi
648 orthogonal array. Mater Des 63: 789-797. DOI: 10.1016/j.matdes.2014.07.003

649 Wang L, Liang W, Yu J, Liang Z, Ruan L, Zhang Y (2013) Flocculation of Microcystis
650 aeruginosa using modified larch tannin. Environ Sci Technol 47(11): 5771-5777. DOI:
651 10.1021/es400793x

652 Wang Y, Xie W (2010) Synthesis of cationic starch with a high degree of substitution in
653 an ionic liquid. CarbohydrPolym 80(4): 1172-1177. DOI: 10.1016/j.carbpol.2010.01.042

654 Xie Y, Yan B, Xu H, Chen J, Liu Q, Deng Y, Zeng H (2014) Highly regenerable mussel-
655 inspired Fe3O4@ polydopamine-Ag core–shell microspheres as catalyst and adsorbent
656 for methylene blue removal. ACS Appl Mater Interfaces 6(11): 8845-8852. DOI:
657 10.1021/am501632f

Xu Y, Wu YJ, Sun PL, Zhang F, Linhardt RJ, Zhang AQ (2019) Chemically modified polysaccharides: Synthesis, characterization, structure activity relationships of action. Int J BiolMacromol132: 970-977. DOI: 10.1016/j.ijbiomac.2019.03.213

Yan L, Tao H, Bangal PR (2009) Synthesis and flocculation behavior of cationic cellulose prepared in a NaOH/urea aqueous solution. Clean–Soil Air Water 37(1): 39-44. DOI: 10.1002/clen.200800127

Yang WP, Tarng YS (1998) Design optimization of cutting parameters for turning operations based on the Taguchi method. J Mater Process Technol 84(1-3): 122-129. DOI: 10.1016/S0924-0136(98)00079-X

Yan L, Tao H, Bangal PR (2009) Synthesis and flocculation behavior of cationic cellulose prepared in a NaOH/urea aqueous solution. Clean–Soil Air Water 37(1): 39-44. DOI: 10.1002/clen.200800127

Yuen SN, Choi SM, Phillips DL, Ma CY (2009) Raman and FTIR spectroscopic study of carboxymethylated non-starch polysaccharides. Food Chem. 114(3): 1091-1098. DOI: 10.1016/j.foodchem.2008.10.053

Zhang H, Wang JK, Wang R, Dong YC (2013) Microwave irradiated synthesis of grafted cationic starch: Synthesis, characterization, application, and biodegradation. J Appl Polym Sci 130(3): 1645-1652. DOI: 10.1002/app.39310

Figures

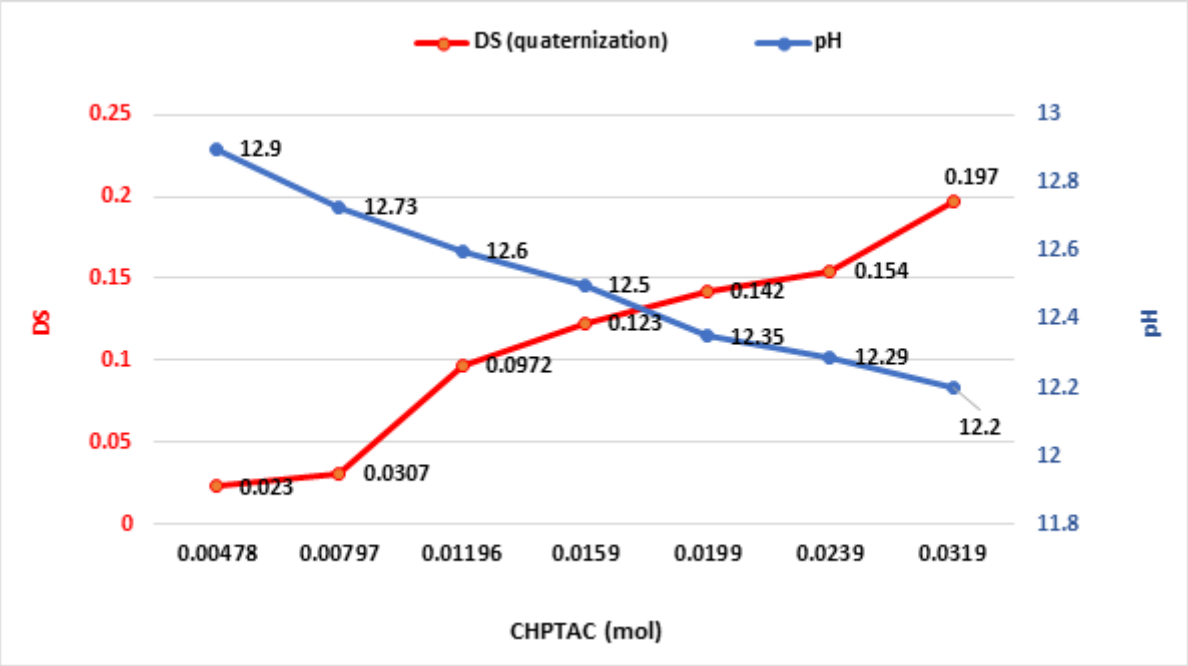

Figure 1

Effect on DS (quaternisation) and pH on varying amount of CHPTAC

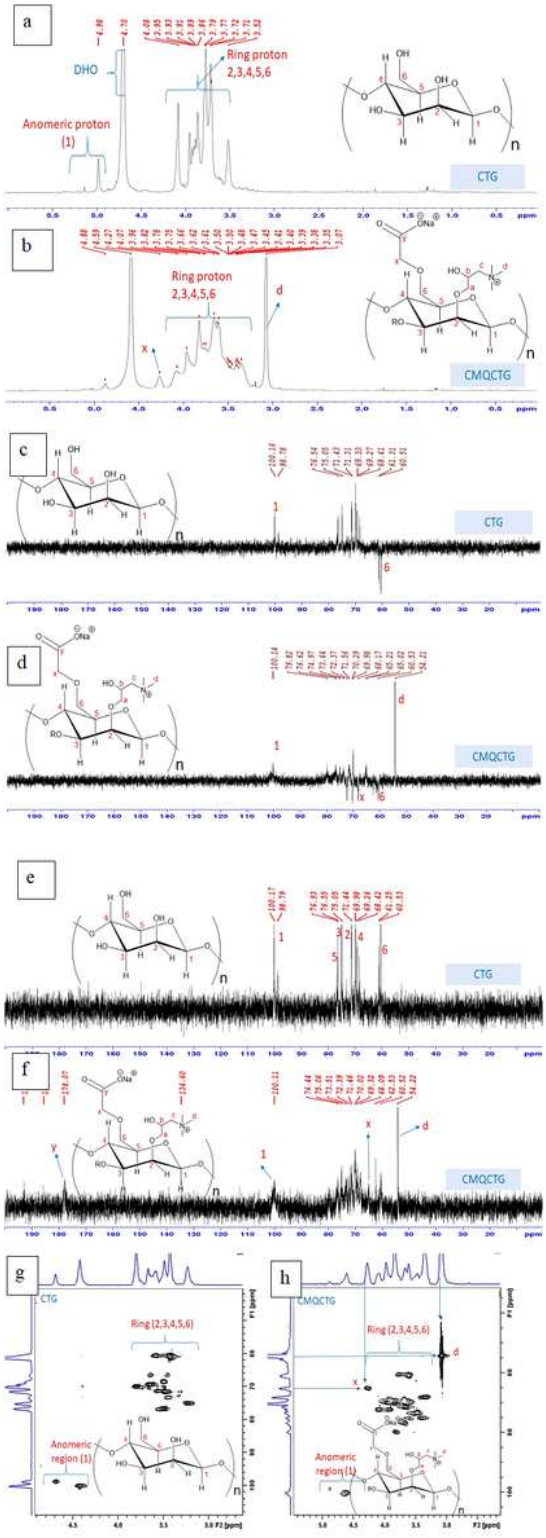

Figure 2

NMR spectrum of CTG and CMQCTG: (a& b) 1H-NMR spectrum; (c & d) 13C-NMR spectrum; (e & f) DEPT Spectrum; (g & h) HSQC Spectrum

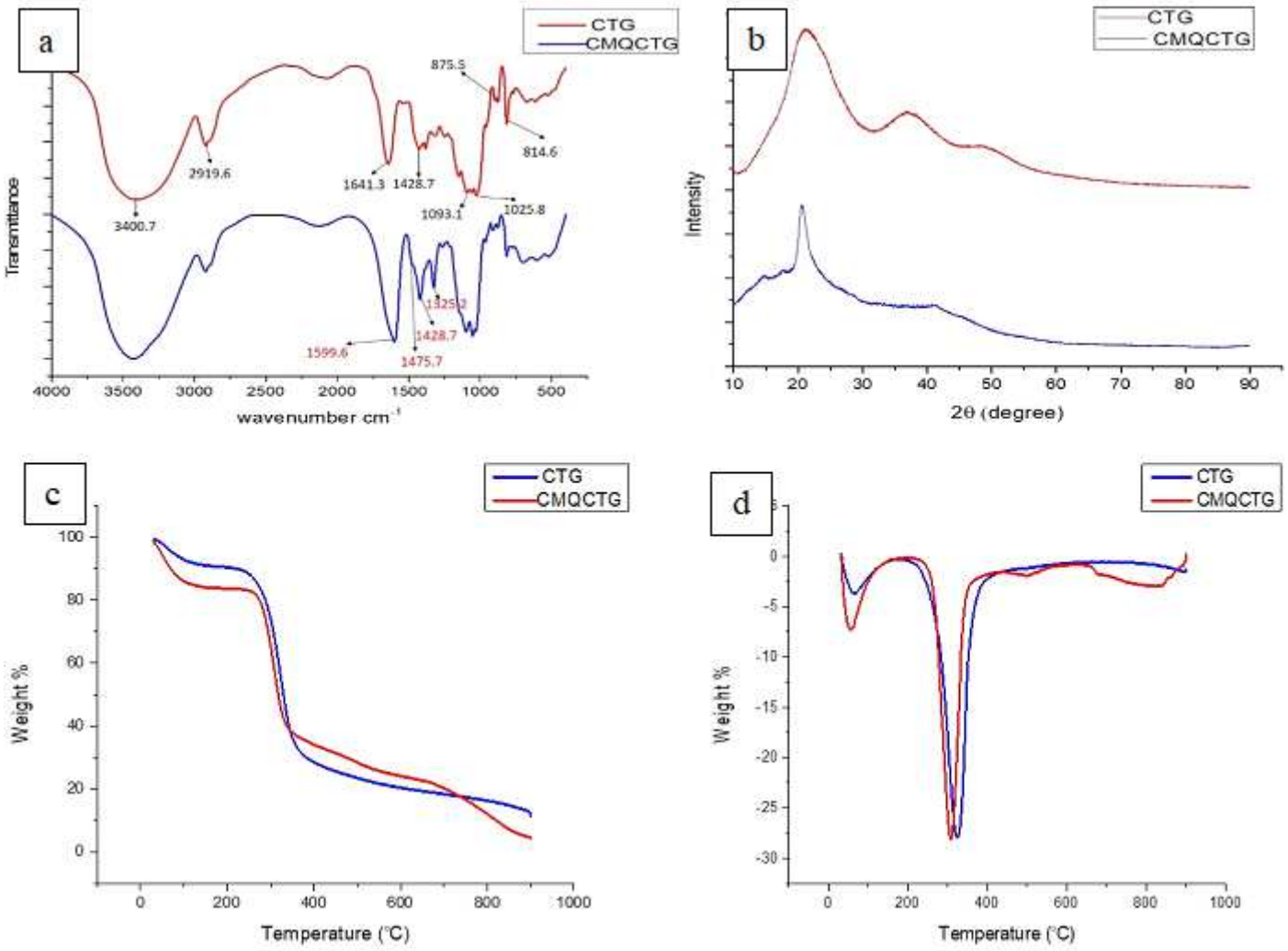

Figure 3

(a) FT-IR spectra of CTG & CMQCTG (b) XRD of CTG and CMQCTG (c) TGA of CTG & CMQCTG (d) DTG of CTG & CMQCTG

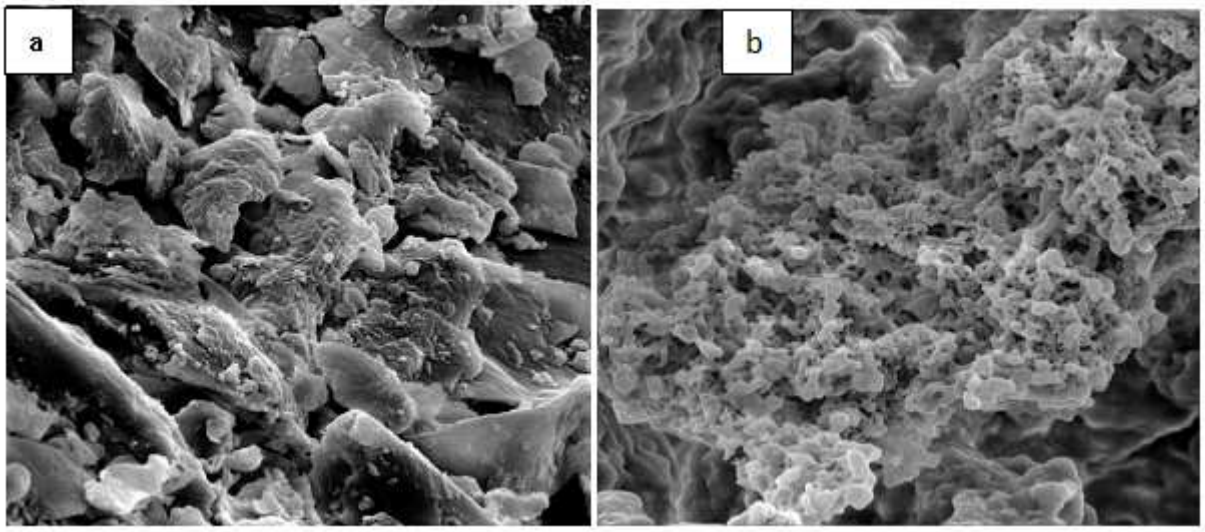

Figure 4

(a) FESEM image of (a) CTG and (b) CMQCTG

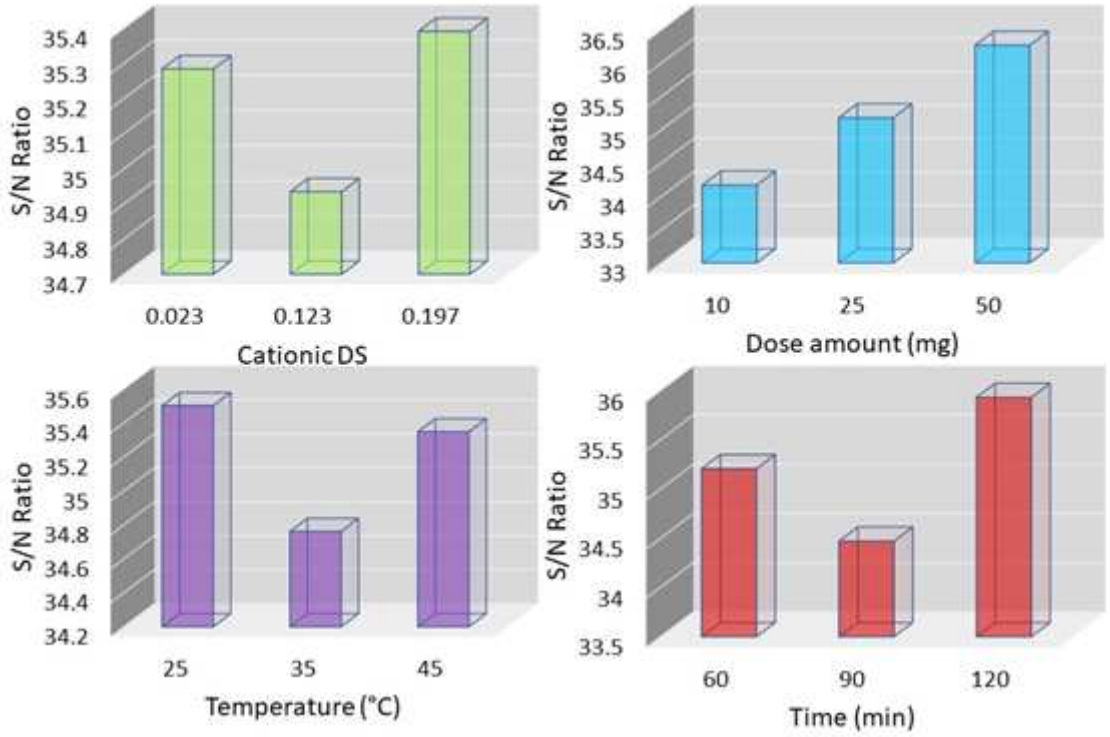

Figure 5

Effect of different parameters on Malachite Green dyes with respect to S/N ratio

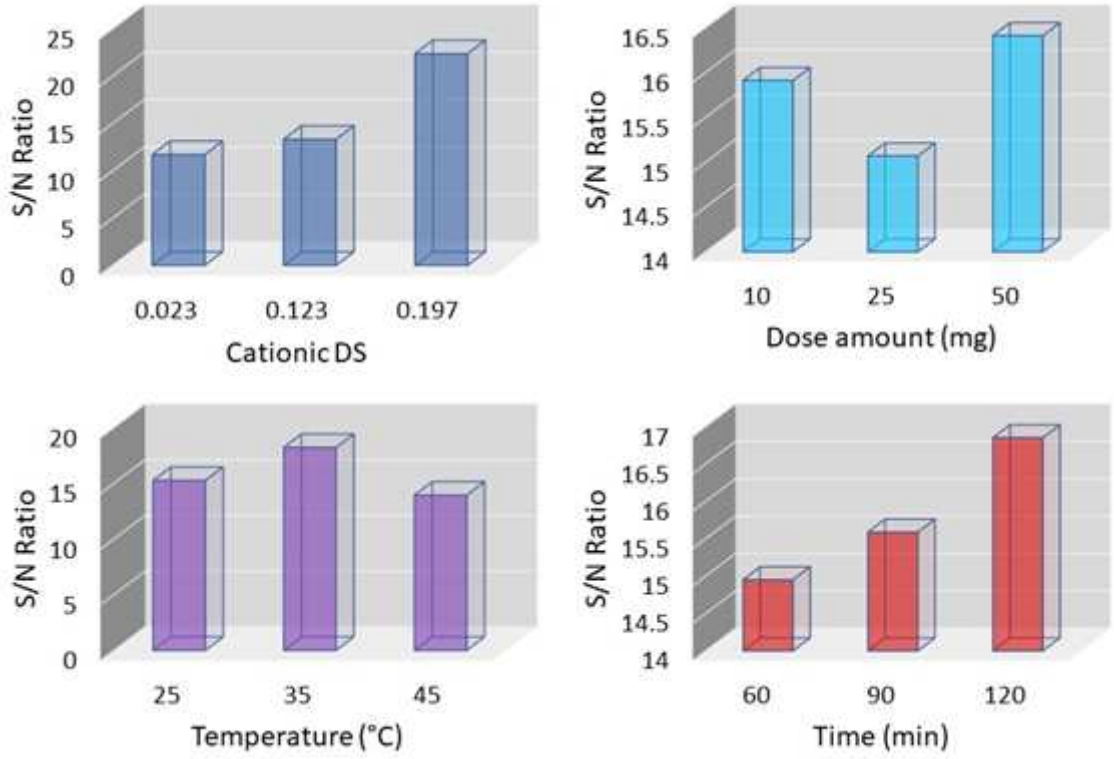

Figure 6

Effect of different parameters on Congo Red dyes with respect to S/N ratio

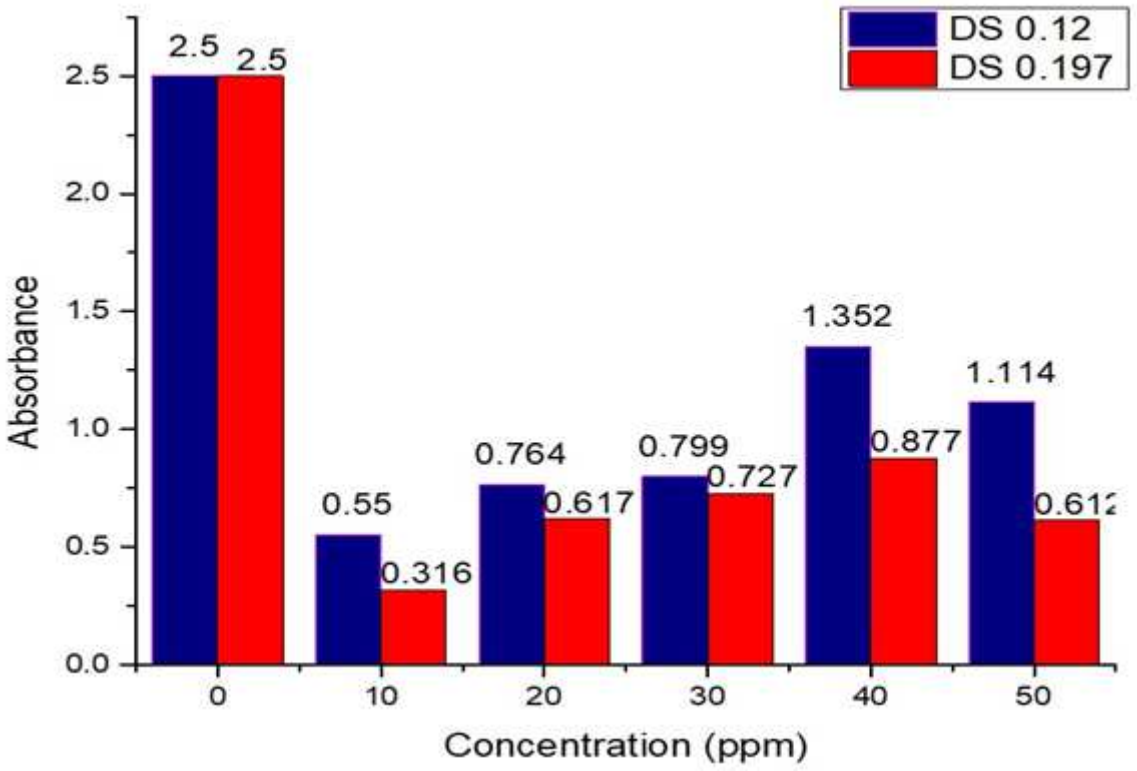

Figure 7

Flocculation performance of CMQCTG

Supplementary Files

This is a list of supplementary files associated with this preprint. Click to download.

- Scheme01.png